

Synergism in the Antibacterial Action of Ternary Mixtures Involving Silver Nanoparticles, Chitosan and Antibiotics

Marcelo S. L. Brasil,^a Aline L. Filgueiras,^a Marina B. Campos,^b Mariana S. L. Neves,^b
Mateus Eugênio,^c Lídia A. Sena,^d Celso B. Sant'Anna,^c Vânia L. da Silva,^b
Cláudio G. Diniz^b and Antonio C. Sant'Ana^{*,a}

^aLaboratório de Nanoestruturas Plasmônicas, Departamento de Química, Universidade Federal de Juiz de Fora, 36036-900 Juiz de Fora-MG, Brazil

^bLaboratório de Fisiologia e Genética Molecular Bacteriana, Instituto de Ciências Biológicas, Universidade Federal de Juiz de Fora, 36036-900 Juiz de Fora-MG, Brazil

^cDiretoria de Metrologia Aplicada às Ciências da Vida, Instituto Nacional de Metrologia, Qualidade e Tecnologia, 20261-232 Rio de Janeiro-RJ, Brazil

^dDiretoria de Metrologia Científica e Tecnológica, Instituto Nacional de Metrologia, Qualidade e Tecnologia, 20261-232 Rio de Janeiro-RJ, Brazil

The investigations of the antibacterial actions, observed in ternary associations involving silver nanoparticles (AgNPs), chitosan and the antibiotics azithromycin (AZ), levofloxacin (LE) or tetracycline (TE), against Gram-negative and Gram-positive bacterial strains, were performed by *in vitro* antimicrobial susceptibility testing and checkerboard assays. The pH impact in the culture medium was carefully discarded, but preserving the best conditions for solubilizing chitosan. The synergistic antibacterial effects were observed in the most combinations of AgNPs, chitosan and antibiotic, leading to a reduction from 37 to 97% in the minimum inhibitory concentration of the drugs. The mechanisms for the enhanced antimicrobial effects were proposed based on the investigations of the adsorptions of the drugs on the silver surfaces through surface-enhanced Raman scattering (SERS) spectroscopy.

Keywords: surface chemistry, Ag⁺ ion, LSPR spectroscopy

Introduction

Silver nanomaterials have attracted significant interest from chemists, biochemists, physicists and medical experts by reflecting the extraordinary functional properties and increasingly numerous applications in biomedical technology.^{1,2} The early reports of the medicinal use of silver salts date centuries before the discovery of antibiotics in the first half of 20th century.^{3,4} Antibiotics play important role in clinical treatment, but their overuse resulted in a loss of efficiency due to the development and spreading of antibiotic-resistant bacteria,⁵ leading to a renewed interest in the antimicrobial properties of silver compounds. It was enhanced by the recent advances in the production of silver nanostructures with fine control of its chemical surface properties.^{6,7} In addition, such nanomaterials can be used as

substrates for surface-enhanced Raman scattering (SERS) spectroscopy, with several applications in biochemistry and medicine.^{8,9} A question whose answer can lead to a novel scenery is how silver nanoparticles (AgNPs) can be combined with antibiotics to face bacterial resistance.

The mechanisms of antimicrobial action of the most silver salts, as well as of the nanostructured silver, were only partially elucidated, revealing multiple actions. It has been proposed that ionic silver interacts inside the cell with multiple target sites, as phosphorus and sulfur compounds,¹⁰ whose alterations lead to eventually chemical modifications of proteins and nucleic acids and metabolic disruption due to the interruption of respiratory electron transport chain.¹¹ It has been suggested that once sufficient ionic silver has undergone uptake by bacterial cell, its survival is improbable.¹² AgNPs can present enhanced antimicrobial response since they can release silver ion from the oxidative process on the metallic surface, but

*e-mail: antonio.sant@ufjf.edu.br

also present other mechanisms of action. The affinity of AgNPs with diameter around 1-10 nm by the bacterial cell wall can lead to the formation of pores with cytoplasmic leakage and cell death.^{11,13-15} Internalized metallic silver can catalyze the formation of reactive oxygen species in cytoplasmic medium, leading to oxidative stress with metabolic disruption.^{10,16} The control of the size and shape of AgNPs can be performed varying kinetic parameters and stabilizing agents in the syntheses and the final size distributions directly influence antimicrobial activities. The challenge is to tune such geometric parameters of AgNPs, in nanometer scale, to control their antimicrobial effects.¹⁷⁻²⁰

Chitosan is a biodegradable and biocompatible copolymer of *N*-acetyl-D-glucosamine and D-glucosamine that presents antimicrobial activity. Such macromolecules showed high capacity to stabilize and prevent aggregation of AgNPs in aqueous medium, due to the strong coordinative interaction involving amine groups and silver atoms.²¹ The preservation of the sizes of the AuNPs is a meaningful issue to be considered for studying their interactions in biological medium. In the solid state chitosan is semi crystalline, insoluble in water at neutral pH and readily soluble in acidic solutions.²²⁻²⁵ Chitosan is a Lewis base, with primary amino groups protonated in acidic conditions, with a pK_a value of 6.3.²⁶ The most common medium used for solubilizing chitosan is acetic acid (HAc) aqueous solution in the concentration of 1% v/v (percentage in volume fraction), whose pH is ca. 3.0. It is also soluble in aqueous solutions of hydrochloric or nitric acids, but insoluble in sulfuric and phosphoric acids.^{26,27} Chitosan has shown a low toxicity for human cells,^{28,29} and its antimicrobial activity is largely dependent on the molecular weight, the degree of deacetylation,³⁰ and involves the destabilization of the negatively-charged bacterial cell wall by the electrostatic interactions with the positively-charged protonated polymer chains.^{17,29} Such antimicrobial mechanism is similar to the described for AgNPs and their conjugated use results in synergism.¹⁷

The efficiency of silver salts and AgNPs as bactericides can be increased by combining them to other organic antimicrobial agents, as polymers and antibiotics, with several records of synergism.^{31,32} Kora and Rastogi³³ observed antibacterial activity of AgNPs capped with citrate, sodium dodecylsulfate and polyvinylpyrrolidone combined with streptomycin, ampicillin, and tetracycline, which were evaluated with Gram-negative and Gram-positive bacteria, employing a disc diffusion assay. Shahverdi *et al.*³⁴ investigated the synergistic antibacterial effect for the combination of AgNPs with fourteen antibiotics. Hwang *et al.*³⁵ studied the combined effects between AgNPs and the antibiotics ampicillin, chloramphenicol and kanamycin against several

pathogenic bacteria, observing synergistic effect. De Oliveira *et al.*³⁶ showed AgNPs protected with a silica shell modified with ampicillin presenting synergistic effect against antibiotic-resistant *E. coli*.

In this work, chitosan-stabilized silver nanoparticles (AgNP-Chit) were synthesized to achieve narrow size distribution, high stability with unimportant aggregation process, and high metal concentration. Antibacterial activities were then evaluated for AgNP-Chit and its combination with the antimicrobial drugs azithromycin (AZ), levofloxacin (LE) and tetracycline (TE). These systems were tested against different bacterial strains: Gram-negative *Escherichia coli* and *Klebsiella pneumoniae*, and Gram-positive *Staphylococcus aureus* and *Enterococcus faecalis*. The combinatory effects involving AgNP-Chit and the drugs were evaluated, by using the checkerboard method, to determine the presence of synergistic effects. The proposals for the mechanisms of the improved antimicrobial actions were constructed based on the analysis of the adsorption of the drugs on the silver surface through SERS spectroscopy.

Experimental

Silver nitrate, sodium borohydride, trisodium citrate, HAc, AZ, TE, LE, NaOH, Mueller Hinton culture media and chitosan (low molecular weight) were purchased from Sigma-Aldrich. Deionized water with ultrapure pattern (18.2 M Ω cm resistivity, Milli-Q) was used in the synthesis of AgNPs and AgNP-Chit. All materials were autoclaved or filter-sterilized for further aseptic working conditions in the biological tests.

AgNPs aqueous suspension was synthesized by the dropwise addition of 0.5 mL of 1.26 mol L⁻¹ sodium borohydride aqueous solution to 50.0 mL of 2.1 $\times 10^{-3}$ mol L⁻¹ of silver nitrate aqueous solution at 25 °C, with continuous stirring. An aliquot of 5 mL of 2.2 g L⁻¹ of chitosan solubilized in 1% v/v HAc aqueous medium was added dropwise to AgNPs aqueous suspension, under continuous stirring, to produce AgNP-Chit. Both AgNPs and AgNP-Chit colloidal suspensions were used in the antibacterial assay, as described below. The final concentrations of silver and chitosan in the AgNP-Chit suspension were ca. 0.2 g L⁻¹. The pH of both AgNP-Chit and chitosan aqueous suspensions were adjusted by using 1.0 mol L⁻¹ NaOH aqueous solution.^{37,38}

The minimum inhibitory concentration (MIC) values were determined through broth dilution technique in microtiter plates in accordance to the Clinical and Laboratory Standards Institute (CLSI) guidelines³⁹ for each compound: Ag⁺ ion, AgNPs, chitosan, AgNP-Chit and the antimicrobial drugs (AZ, LE and TE) against two

Gram-negative bacteria *Escherichia coli* (ATCC 11229) and *Klebsiella pneumonia* (ATCC 700603), and two Gram-positive strains *Staphylococcus aureus* (ATCC 29213) and *Enterococcus faecalis* (ATCC 51299).

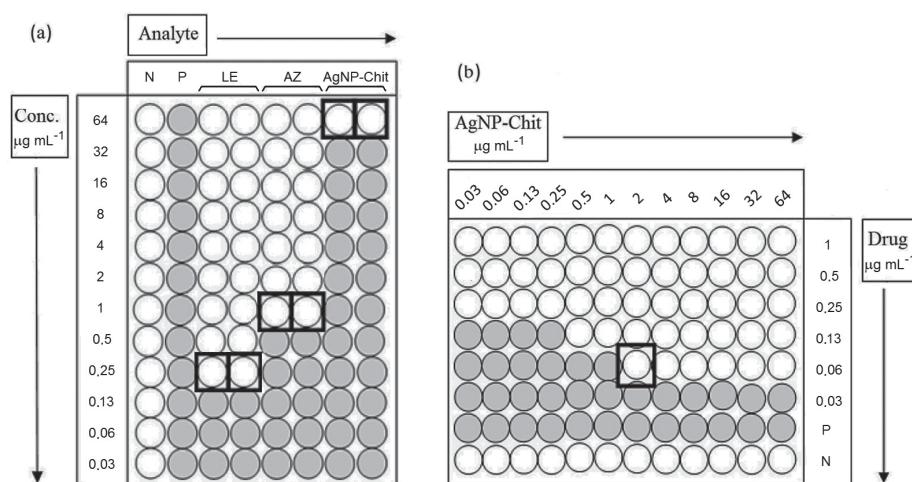
In the MIC tests, the bacterial suspension 0.5 McFarland (approximately 10^8 colony forming units *per* mL) were prepared from previously aerobically grown bacteria in Mueller Hinton agar, at 37 °C, for 24 h. In a polystyrene microtiter plate, it was added 150 μ L of bacteria suspension and 150 μ L of the antibacterial agent solution, both diluted in Mueller Hinton broth. The compound concentrations ranged from 0.03 to 64 μ g mL⁻¹. The plates were incubated for 24 h and the bacteria growth was determined by turbidity and color change in the system by adding 0.01 g L⁻¹ resazurin aqueous solution, a non-enzymatic marker. Under viable bacteria metabolism, resazurin turns from dark blue to transparent due to its reduction.⁴⁰

Scheme 1a shows the example of an MIC test, where in the column N is shown the negative test, to be sure that the culture medium was not contaminated, the column P is the positive test, to see that the culture medium promoted the growth of the microorganism and in the other columns are shown, in duplicate, the tests of each agent. The white and gray colors represent the absence or presence of turbidity of the culture medium, respectively, whose existence was a signal of the growth of the microorganism. In the MIC test, the concentration of the antibacterial agents decreased to half, line by line of the culture plate. All tests were repeated one more time and generally the fourfold result presented the same concentration values. In this way, in accordance with the CLSI guidelines,³⁹ the confidence interval can be considered as the concentrations values right below and above of the obtained result.

The checkerboard method was used to achieve the fractional inhibitory concentration index (FIC_{index}) to evaluate if the combinations of AgNP-Chit with antimicrobial drugs would result in synergism. For this assay, as showed in the Scheme 1b, the antibiotics drugs were serially diluted along the vertical wells, while the AgNP-Chit suspension was diluted along the horizontal ones. In the Scheme 1, the line P is the positive test, while the line N is the negative test. The plates were aerobically incubated, at 37 °C, for 24 h and the MIC in the combinations were read as the lowest dilution without any turbidity. Resazurin was also added as a colorimetric aid to determine the absence of bacterial growth.

The FIC_{index} was used to interpret the results and was calculated as follows: $FIC_{index} = FIC_a + FIC_b$, where $FIC_a = MIC_{a-c}/MIC_a$ and $FIC_b = MIC_{b-c}/MIC_b$, where $MIC_{a,b}$ is the minimum inhibitory concentration of the antimicrobial agent alone and $MIC_{a,b-c}$ is the minimum inhibitory concentration of the antimicrobial in combination in the checkerboard test. The index “a” was used for AgNP-Chit and the index “b” for each antibiotic. The effect in the combination was considered synergistic when $FIC_{index} \leq 0.5$, additive when $0.5 < FIC_{index} < 1$, while the antagonism was considered if $FIC_{index} \geq 4$.⁴¹⁻⁴³

The UV-Vis spectra of chitosan and AgNPs suspensions were performed in UV-1800 Shimadzu spectrophotometer, using 0.1 cm path length quartz cuvette in ultraviolet-visible range. Scanning electron microscopy (SEM) image was taken using an FEI high-resolution field-emission gun scanning electron microscope (FEG-SEM), Magellan 400, by dropwise the colloidal suspension on a silicon plate, without previous centrifugation or dilution. The transmission electron microscopy (TEM)



Scheme 1. (a) MIC test with concentrations varying in the lines and analytes in the columns (in duplicate); (b) checkerboard test with the concentrations of AgNP-Chit varying in the columns and the concentrations of one determined antibiotic varying in the lines. Gray circles represent the turbidity of the medium due to the growth of the microorganisms. The bold squares indicate the point of the MIC lectures. N and P represent the negative and positive tests, respectively.

images were obtained for *Staphylococcus aureus* and *Klebsiella pneumoniae* untreated and treated with AgNP-Chit. They were collected by centrifugation, washed in PBS (phosphate-buffered saline), fixed in 2.5% v/v glutaraldehyde and 4% v/v paraformaldehyde in 0.1 mol L⁻¹ phosphate buffer, pH 7.2, post fixed in 1.0 g L⁻¹ osmium tetroxide, 0.8 g L⁻¹ potassium ferrocyanide, 5.0 mmol L⁻¹ calcium chloride in 0.1 mol L⁻¹ cacodylate buffer, pH 7.2, dehydrated in an increasing acetone series and embedded in Epon resin. Ultrathin sections were stained with uranyl acetate and lead citrate and observed in an FEI Tecnai Spirit 12 transmission electron microscope operating at 80 kV. Dynamic light scattering (DLS) and zeta potential were measured using a Zetasizer Nano ZS, Zetasizer Nano ZS, Malvern Instruments. The Raman spectra of the antibiotics in solid state were obtained in an RFS-100 Bruker spectrometer, with Nd-YAG laser line emitting at 1064 nm, equipped with a Ge-detector cooled with liquid nitrogen, laser power at 100 mW. The SERS spectra of the drugs was obtained in an inVia Renishaw spectrometer, coupled with an Olympus microscope with a 50× objective lens, using exciting radiation with wavelength at 532 nm. The SERS spectra were collected in aqueous medium, at 1.0 × 10⁻³ mol L⁻¹, with laser power at 2 mW.

Results and Discussion

The solubility of chitosan was evaluated by UV-Vis spectroscopy using different acids and pH conditions (for more details see Figures S1 and S2, Supplementary Information (SI) section), and acetic acid 1% v/v was chosen as the solubilization medium. The impact of the pH of chitosan suspension have to be considered in false positive results in the antimicrobial tests, since high or low pH of the culture medium can lead to an increase in the rate of inactivation of the cellular enzymes.⁴⁴ There is a range of pH near neutral condition for the growth of the most bacteria that do not affect the rate of growth and survival of the microorganisms, though this discussion involving the antimicrobial action of chitosan solubilized in HAC is rare.^{21,45} The pH of the original aqueous suspension of chitosan in HAC 1.0% v/v, was adjusted with 1.0 mol L⁻¹ NaOH aqueous solution, by adding dropwise under mechanical stirring. Figure 1 presents the UV-Vis spectra of these aqueous suspensions in different pH for monitoring the threshold of the chitosan solubilization.

The UV-Vis spectrum of chitosan suspension at pH 6.5 shows higher baseline signal, ascribed to the enhancing of scattering associated with the greater average particle size, which was caused by the loss of the best solubility condition of the polymer in the aqueous medium. Since the

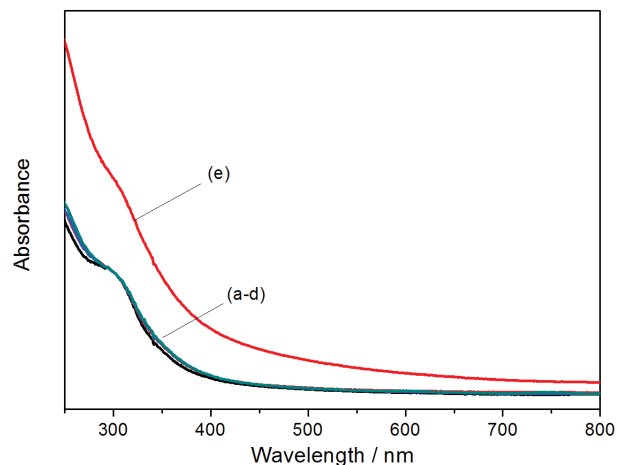


Figure 1. UV-Vis spectra of chitosan aqueous suspension in HAC medium in different adjusted pH values: (a) 3.0; (b) 5.0; (c) 5.5; (d) 6.0 and (e) 6.5.

pK_a of chitosan is 6.3, such lower solubility was expected. Thus, pH 6.0 was the higher one that did not affect the chitosan solubility and was chosen as the pH condition for the AgNP-Chit suspension used in the biological tests.

Figure 2 presents the UV-Vis spectrum and the SEM micrograph of AgNP-Chit aqueous suspension after the pH adjustment to 6.0. The localized surface plasmon resonance band, assigned to the silver nanostructures, is narrow and has a maximum at 390 nm. These spectral patterns are assigned to the presence of small AgNPs, with typical dimension of ca. 5-30 nm that makes this system suitable for biological assays.^{46,47} The SEM micrograph of AgNP-Chit and its size distribution obtained by dynamic light scattering confirm that the diameters vary in this range, with the most probable values around 15 nm. The pH adjustment of the suspension did not change the size of AgNPs (see Figure S3, SI section). It is noteworthy the high stability of AgNPs recovered with chitosan in aqueous medium, which can be preserved without aggregation by months. The values of the zeta potential from AgNP-Chit suspension was 41 ± 1 mV indicating the protonated chitosan chains are near the metallic surfaces, strongly interfering in the surface charge of the AgNP.

Some experiments with the pH of the culture medium varying from pH 6.0 to 7.0 were carried out, and the growth patterns of the bacteria in this pH range did not change. Only when the pH decreased to 5.0 or less, the growth of the bacteria was affected (see Tables S1-S3, SI section). In this way, the pH 6.0 was the best choice for using in the biological tests and for stabilizing the AgNP-Chit aqueous suspension, for excluding the antimicrobial action in the acidic medium.

Table 1 shows the susceptibility patterns of AgNPs, AgNP-Chit, the drugs and all other species used in the syntheses of the colloidal suspensions tested against

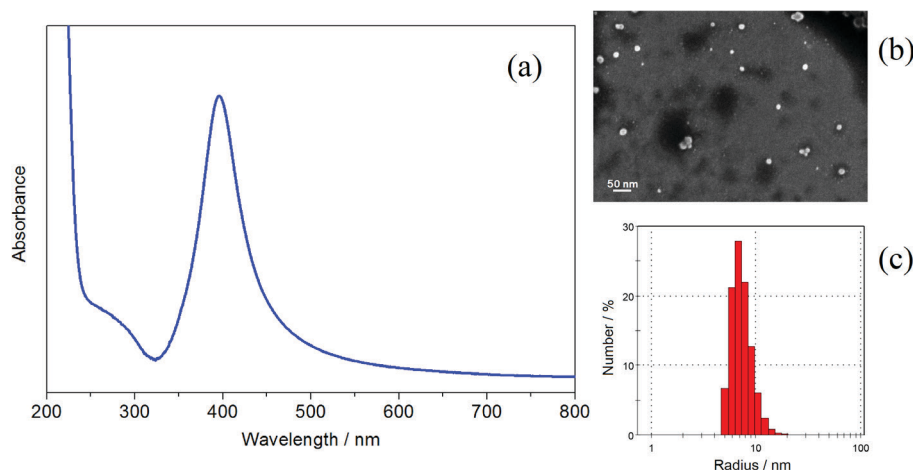


Figure 2. (a) UV-Vis spectrum of AgNP-Chit aqueous suspension at pH 6.0; (b) SEM micrograph of AgNP-Chit dried on silicon plate; (c) size distribution of AgNP-Chit obtained by DLS measurements.

Table 1. MIC values of the isolated antibacterial agents: Ag⁺ ion, AgNPs, AgNP-Chit, antibiotics, and all other components used in the syntheses of colloids, acting against Gram-negative and Gram-positive bacterial strains

Tested agent	<i>E. coli</i> (ATCC 11229) ^a		<i>S. aureus</i> (ATCC 29213) ^b	
	MIC _{Bacteriostatic} / (μg mL ⁻¹)	MIC _{Bactericide} / (μg mL ⁻¹)	MIC _{Bacteriostatic} / (μg mL ⁻¹)	MIC _{Bactericide} / (μg mL ⁻¹)
Ac ^{-c}	> 128.0 ^d	> 128.0 ^d	> 128.0 ^d	> 128.0 ^d
Ag ⁺	16.0	32.0	16.0	16.0
BH ₄ ⁻	> 1408.0 ^d	> 1408.0 ^d	> 1408.0 ^d	> 1408.0 ^d
Chitosan ^c	176.0	176.0	176.0	704.0
AZ	0.25	0.25	1.0	1.0
LE	0.5	1.0	0.25	0.25
TE	0.5	1.0	1.0	1.0
AgNPs	> 128.0 ^d	> 128.0 ^d	> 128.0 ^d	> 128.0 ^d
AgNP-Chit ^c	32.0	32.0	32.0	64.0

^aGram-negative bacteria; ^bGram-positive bacteria; ^cpH adjusted to 6.0; ^dthe first concentration of the MIC plate. MIC: minimum inhibitory concentration; AZ: azithromycin; LE: levofloxacin; TE: tetracycline. MIC (μg mL⁻¹) values informed in CLSI,³⁹ for *S. aureus* (ATCC 29213) are AZ 0.5-2; LE 0.06-0.5; TE 0.12-1.0, but these antibiotics acting against *E. coli* (ATCC 11229) are not informed in this database.

Gram-negative *E. coli* and Gram-positive *S. aureus* bacteria, including bactericidal and bacteriostatic effects.

The antibacterial activities of borohydride, acetate, chitosan and AgNPs were small. However, AgNP-Chit shows significant antibacterial effect, which is comparable with silver nitrate. The FIC_{index} values for such a combination was 0.34 for both bacterial strains, showing that synergistic effect is present. The MIC values for the antibiotics presented in the Table 1 are in agreement with CLSI patterns,³⁹ which allowed the expansion of the screening for two additional bacterial strains in the following checkerboard assays.

Table 2 shows the susceptibility patterns in checkerboard test of the Gram-negative and Gram-positive bacterial strains tested against the combinations of AgNP-Chit and antibiotics with the respective calculated FIC_{index} values.

Synergistic interactions involving the combinations of AgNP-Chit and all antibiotics were observed against both *E. coli* and *E. faecalis*. Synergism was also present in the assays with *S. aureus* when AgNP-Chit was in combination with AZ and TE, as well as *K. pneumoniae* with AgNP-Chit and LE. The additive effects were present when LE and AgNPs were used against *S. Aureus* and TE with AgNPs against *K. pneumoniae*. It is important to note that the antagonistic effect was not observed. The reductions of the doses of each antibiotic, when tested in the ternary combination, were significant for all bacterial strains. As an example, in the experiment involving *S. Aureus* the MIC values for both AZ alone (Table 1) and in the ternary combination were 1.0 and 0.031, respectively, showing a reduction of 97% in the doses of this drug.

Table 2. MIC values for each antibiotic, in combination with AgNP-Chit, acting against Gram-negative and Gram-positive bacteria, and their corresponding FIC values

Antibiotic	MIC _{a,c} ; MIC _{b,c} / ($\mu\text{g mL}^{-1}$)	MIC _a ; MIC _b / ($\mu\text{g mL}^{-1}$)	FIC _a ; FIC _b / ($\mu\text{g mL}^{-1}$)	FIC _{index} / ($\mu\text{g mL}^{-1}$)
<i>E. coli</i> (ATCC 11229) ^a				
AZ	0.06; 0.03	32.0; 0.25	0.002; 0.156	0.158
LE	1.0; 0.13	32.0; 0.5	0.03; 0.25	0.28
TE	1.0; 0.06	32.0; 0.5	0.03; 0.13	0.16
<i>K. pneumoniae</i> (ATCC 700603) ^a				
LE	0.06; 0.5	32.0; 1.0	0.002; 0.48	0.482
TE	8.0; 8.0	32.0; 16.0	0.25; 0.50	0.75
<i>S. Aureus</i> (ATCC 29213) ^b				
AZ	0.06; 0.03	32.0; 1.0	0.002; 0.031	0.033
LE	1.0; 0.13	32.0; 0.25	0.03; 0.63	0.66
TE	1.0; 0.06	32.0; 1.0	0.03; 0.06	0.09
<i>E. faecalis</i> (ATCC 51299) ^b				
LE	0.06; 0.5	16.0; 1.0	0.004; 0.48	0.484
TE	0.06; 0.5	16.0; 4.0	0.004; 0.12	0.124

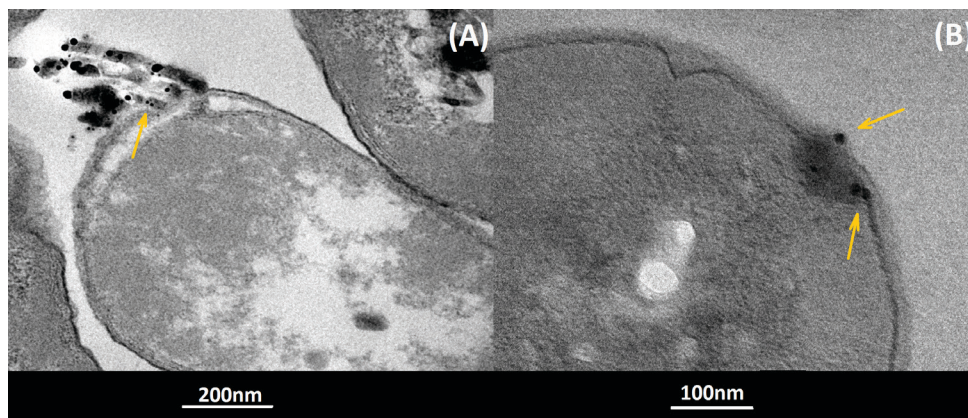
^aGram-negative bacteria; ^bGram-positive bacteria. MIC_{a,c}: minimum inhibitory concentration (MIC) of the AgNP-Chit in combination in the checkerboard test; MIC_{b,c}: MIC of the antibiotics in combination in the checkerboard test; MIC_a: MIC of AgNP-Chit; MIC_b: MIC of the antibiotics; FIC_a: fractional inhibitory concentration of AgNP-Chit; FIC_b: fractional inhibitory concentration of the antibiotics; FIC_{index}: fractional inhibitory concentration index; AZ: azithromycin; LE: levofloxacin; TE: tetracycline. For the FIC calculations, the MIC_{a,c} were divided by bacteriostatic MIC_a from Table 1. MIC ($\mu\text{g mL}^{-1}$) values informed in CLSI,³⁹ for *E. faecalis* (ATCC 51299) are AZ n/a; LE 0.25-2; TE 8-32, but these antibiotics acting against *K. pneumoniae* (ATCC 700603) are not informed in this database.

Figure 3 shows TEM micrographs of Gram-negative *K. pneumoniae* and Gram-positive *S. aureus* bacteria treated with AgNP-Chit, after the incubation in similar conditions of the MIC analyses. The presence of AgNP-Chit led to a large number of lysed cells, and such nanoparticles were observed near the cellular membrane, sometimes changing its morphology, as indicated by arrows in Figure 3. Such interactions led to changes in the stability of bacterial membranes and walls (see Figures S4 and S5, SI section), and can be involved in the mechanism of the lysis process. The interactions of positively charged chitosan with the overall negatively charged surface of the bacteria are described in the literature as the main mechanism involved in the antibacterial activity.^{15,21} In the same way, the formation of pores in the

bacterial cell wall by the positive low charged AgNP surfaces is described as the cause of the lyses of the cells.^{11,47} Both mechanisms can be ascribed to the synergism here observed.

The synergism observed in the checkerboard assays when ternary combinations of AgNP-Chit with the antibiotics AZ, LE and TE were used, which showed reductions of the drug doses higher than 70% in the most experiments, can be rationalized assuming that the affinities of the drugs for the metallic surfaces led the AgNP-Chit works as carriers of drugs. This hypothesis was investigated by Raman and SERS spectroscopy and the spectra are presented in the Figure 4.

The remarkable differences observed between the Raman spectra of the solids and the SERS spectra of the adsorbed

**Figure 3.** TEM micrographs of (A) *K. pneumoniae* and (B) *S. aureus* treated with AgNP-Chit.

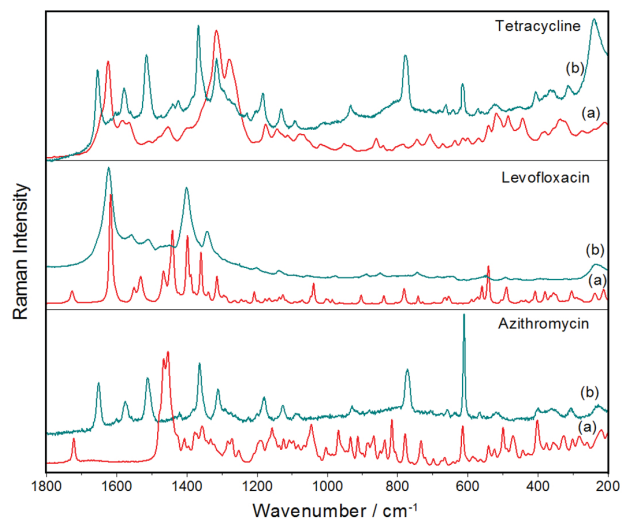


Figure 4. (a) Raman spectra of each antibiotic in solid state, and (b) SERS spectra of the respective compound adsorbed on the silver surfaces of AgNPs substrates. Wavelengths of the respective exciting radiations: 1064 and 532 nm.

molecules can be explained by the high affinity of these compounds by the metallic surface, ascribed to chemical interactions that led to the formation of surface complexes.⁴⁸ Such molecules, stuck on the silver surface, could be carried to the wall of the bacteria, driven by the chemical affinity of the silver by specific sites of proteinaceous structures.

The interpretations of the changes in the spectral patterns allow inferring that tetracycline interacts strongly with silver surface through more than one carbonyl group, while levofloxacin coordinates with silver through carboxylate group.⁴⁸ The SERS spectrum of azithromycin shows significant shifts in the bands at 1651 and 1513 cm^{-1} , assigned to carbonyl modes, with enhancements of their relative intensities, indicating that carbonyl moiety is the probable anchoring site of this molecule on the metallic surface.

The synergic behaviors observed when antibiotics were associated to AgNPs were described in the literature with several drugs. The mechanisms proposed involve the formation of chemical bonds among the antibiotic molecules and the AgNP surfaces, which work as a drug delivery systems.^{31-36,49,50} Such propositions are in agreement with the assumption here presented, since the three used drugs have antibacterial activities involving intracellular interference in the metabolism of DNA or RNA. Their uptakes take place due to the affinity of silver surfaces for the bacterial membranes, probably followed by the release of the antibiotic molecules in the intracellular medium due to the oxidation of the AgNP surfaces. Consequently, the overall synergism from such ternary materials involves the high affinity of chitosan and silver surfaces by the external bacterial walls,^{10,17,51} working as drug delivery systems, which promotes the internalization of the adsorbed

drugs, followed by their release. In parallel, the several mechanisms of actions from both metallic and ionic silver take place, enhancing significantly the cell death.¹¹

Conclusions

Chitosan and AgNPs aqueous suspensions have separately showed low antibacterial effects, but synergy was observed when both components were combined as the binary mixture AgNP-Chit. The different chemical affinities of metallic silver and chitosan for specific sites of the cell wall of the bacteria can be an explanation for such an enhanced antibacterial action. In addition, the majority of the ternary combinations of the antibiotics TE, LE or AZ with AgNP-Chit tested against two Gram-negative and two Gram-positive bacterial strains presented significant synergistic effects with only two situations showing additive effects. It is noteworthy that the diminishments in the antibiotic doses in the combinations were always present and higher than 70% in the most ternary combinations. The antagonistic effect was not observed, and in all assays the control of the pH, kept in 6.0, was actually essential for reliable evaluations of the antibacterial effects of such formulations.

The high affinity of the three antibiotics, TE, LE and AZ, for the silver surface of AgNP-Chit, observed by the analyses of their respective SERS spectra, together with the known affinities of metallic silver and chitosan compounds for the outer wall of bacteria, allowed suggesting AgNP-Chit worked *in vitro* as carriers of these drugs for the tested bacterial strains.

Supplementary Information

Supplementary data (spectra and TEM images) are available free of charge at <http://jbcs.sbq.org.br> as PDF file.

Acknowledgments

The authors would like to thank FAPEMIG (CEX-APQ-02392/15 and CEX-RED-00010-14), CNPq (407279/2013-0) and CAPES, Brazilian financial foundations, for the scholarships, grants and research support. In addition, we would like to thank Embrapa Gado de Leite for zeta potential and DLS measurements.

References

- Zhu, X.; Li, J.; He, H.; Huang, M.; Zhang, X.; Wang, S.; *Biosens. Bioelectron.* **2015**, *74*, 113.
- Banerjee, I.; Pangule, R. C.; Kane, R. S.; *Adv. Mater.* **2011**, *23*, 690.

3. Rai, M.; Yadav, A.; Gade, A.; Aniket, G.; *Biotechnol. Adv.* **2009**, *27*, 76.
4. Edward-Jones, V.; *Lett. Appl. Microbiol.* **2009**, *49*, 147.
5. Huang, M.; Qi, F.; Wang, J.; Xu, Q.; Lin, L.; *J. Hazard. Mater.* **2015**, *298*, 303.
6. Xia, Y.; Xiong, Y.; Lim, B.; Skrabalak, S. E.; *Angew. Chem., Int. Ed.* **2009**, *48*, 60.
7. Jin, R.; Zeng, C.; Zhou, M.; Chen, Y.; *Chem. Rev.* **2016**, *116*, 10346.
8. Wang, Z.; Zong, S.; Wu, L.; Zhu, D.; Cui, Y.; *Chem. Rev.* **2017**, *117*, 7910.
9. Lane, L. A.; Qian, X.; Nie, S.; *Chem. Rev.* **2015**, *115*, 10489.
10. Le Ouay, B.; Stellacci, F.; *Nano Today* **2015**, *10*, 339.
11. Morones, J. R.; Elechiguerra, J. L.; Camacho, A.; Holt, K.; Kouri, J. B.; Ramírez, J. T.; Yacaman, M. J.; *Nanotechnology* **2005**, *16*, 2346.
12. Durán, N.; Marcato, P. D.; Conti, R. D.; Alves, O. L.; Costa, F. T. M.; Brocchi, M.; *J. Braz. Chem. Soc.* **2010**, *21*, 949.
13. Maillard, J.; Hartemann, P.; *Crit. Rev. Microbiol.* **2012**, *39*, 373.
14. Singh, R.; Shedbalkar, U. U.; Wadhvani, S. A.; Chopade, B. A.; *Appl. Microbiol. Biotechnol.* **2015**, *99*, 4579.
15. Eckhardt, S.; Brunetto, P. S.; Gagnon, J.; Priebe, M.; Giese, B.; Fromm, K. M.; *Chem. Rev.* **2013**, *113*, 4708.
16. Jin, J. C.; Wu, X. J.; Xu, J.; Wang, B. B.; Jiang, F. L.; Liu, Y.; *Biomater. Sci.* **2017**, *5*, 247.
17. Cavassin, E. D.; de Figueiredo, L. F. P.; Otoch, J. P.; Seckler, M. M.; de Oliveira, R. A.; Franco, F. F.; Marangoni, V. S.; Zucolotto, V.; Levin, A. S. S.; Costa S. F.; *J. Nanobiotechnol.* **2015**, *13*, article 64.
18. Khurana, C.; Sharma, P.; Pandey, O. P.; Chudasama, B.; *J. Mater. Sci. Technol.* **2016**, *32*, 524.
19. Buszewski, B.; Rafiiska, K.; Pomastowski, P.; Walczak, J.; Rogowska A.; *Colloids Surf., A* **2016**, *506*, 170.
20. Lopez-Serrano, A.; Olivas, R. M.; Landaluze, J. S.; Camara, C.; *Anal. Methods* **2014**, *6*, 38.
21. Regiel, A.; Irusta, S.; Kyzioł, A.; Arruebo, M.; Santamaria, J.; *Nanotechnology* **2013**, *24*, 015101.
22. Ebrahimi, M. M. S.; Schönherr, H.; *Langmuir* **2014**, *30*, 7842.
23. Meyer, C.; Stenberg, L.; Gonzalez-Perez, F.; Wrobel, S.; Ronchi, G.; Udina, E.; Sukanuma, S.; Geuna, S.; Navarro, X.; Dahlin, L. B.; Grothe, C.; Haastert-Talini, K.; *Biomaterials* **2016**, *76*, 33.
24. Zou, P.; Yang, X.; Wang, J.; Li, Y.; Yu, H.; Zhang, Y.; Liu, G. Y.; *Food Chem.* **2016**, *190*, 1174.
25. Pillai, C. K. S.; Paul, W.; Sharma, C. P.; *Prog. Polym. Sci.* **2009**, *34*, 641.
26. Rinaudo, M.; Pavlov, G.; Desbrieres, J.; *Polymer* **1999**, *40*, 7029.
27. Rinaudo, M.; Pavlov, G.; Desbrieres, J.; *Int. J. Polym. Anal. Charact.* **1999**, *5*, 267.
28. Corsi, K.; Chellat, F.; Yahia, L. H.; Fernandes, J. C.; *Biomaterials* **2003**, *24*, 1255.
29. Sanpui, P.; Chattopadhyay, A.; Ghosh, S. S.; *ACS Appl. Mater. Interfaces* **2011**, *3*, 218.
30. No, H.; Park, N.; Lee, S.; Meyers, S.; *Int. J. Food Microbiol.* **2002**, *74*, 65.
31. Habash, M. B.; Park, A. J.; Vis, E. C.; Harris, R. J.; Khursigara, C. M.; *Antimicrob. Agents Chemother.* **2014**, *58*, 5818.
32. Shao, W.; Liu, X.; Min, H.; Dong, G.; Feng, Q.; Zuo S.; *ACS Appl. Mater. Interfaces* **2015**, *7*, 6966.
33. Kora, A. J.; Rastogi, L.; *Bioinorg. Chem. Appl.* **2013**, *2013*, 871097.
34. Shahverdi, A. R.; Fakhimi, A.; Shahverdi, H. R.; Minaian, S.; *Nanomedicine* **2007**, *3*, 168.
35. Hwang, I. S.; Hwang, J. H.; Choi, H.; Kim, K. J.; Lee, D. G.; *J. Med. Microbiol.* **2012**, *61*, 1719.
36. de Oliveira, J. F. A.; Saito, A.; Bido, A. T.; Kobarg, J.; Stassen, H. K.; Cardoso, M. B.; *Sci. Rep.* **2016**, *7*, 1.
37. Aguirre-Loredo, R. Y.; Rodriguez-Hernandez, A. I.; Morales-Sanchez, E.; Gomez-Aldapa, C. A.; Velazquez, G.; *Food Chem.* **2016**, *196*, 560.
38. Sant'Ana, A. C.; Diniz, C. G.; da Silva, V. L.; Neves, M. S. L.; Filgueiras, A. L.; *BR102012027335-A2* **2015**.
39. Clinical and Laboratory Standards Institute (CLSI); M07-A10, *Methods for Dilution Antimicrobial Susceptibility Tests for Bacteria that Grow Aerobically*; CLSI, Wayne, PA, USA, 2015.
40. Taneja, N. K.; Tyagi, J. S.; *J. Antimicrob. Chemother.* **2007**, *60*, 288.
41. Lewis, R.; Diekema, D.; Messer, S.; Pfaller, M.; Klepser, M.; *J. Antimicrob. Chemother.* **2002**, *49*, 345.
42. Odds, F. C.; *J. Antimicrob. Chemother.* **2003**, *52*, 1.
43. Hsieh, M. H.; Yu, C. M.; Yu, V. L.; Chow, J. W.; *Diagn. Microbiol. Infect. Dis.* **1993**, *16*, 343.
44. Padan, E.; Bibi, E.; Ito, M.; Krulwich, T. A.; *Biochim. Biophys. Acta, Biomembr.* **2005**, *1717*, 67.
45. Kumar-Krishnan, S.; Prokhorov, E.; Hernandez-Iturriaga, M.; Mota-Morales, J. D.; Vazquez-Lepe, M.; Kovalenko, Y.; Sanchez, I. C.; Luna-Barcenas, G.; *Eur. Polym. J.* **2015**, *67*, 242.
46. Willets, K. A.; Van Duyne, R. P.; *Annu. Rev. Phys. Chem.* **2007**, *58*, 267.
47. Rizzello, L.; Pompa, P. P.; *Chem. Soc. Rev.* **2014**, *43*, 1501.
48. Filgueiras, A. L.; Paschoal, D.; dos Santos, H. F.; Sant'Ana, A. C.; *Spectrochim. Acta, Part A* **2015**, *136*, 979.
49. Deng, H.; McShan, D.; Zhang, Y.; Sinha, S. S.; Arslan, Z.; Ray, P. C.; Yu, H.; *Environ. Sci. Technol.* **2016**, *50*, 8840.
50. Fayaz, A. M.; Balaji, K.; Girilal, M.; Yadav, R.; Kalaichelvan, P. T.; Venketesan, R.; *Nanomedicine* **2010**, *6*, 103.
51. Sanpui, P.; Murugadoss, A.; Prasad, P. V.; Ghosh, S. S.; Chattopadhyay, A.; *Int. J. Food Microbiol.* **2008**, *124*, 142.

Submitted: February 21, 2018

Published online: April 11, 2018

